Available online at www.sciencedirect.com
ScienceDirect
Polymer 48 (2007) 5107–5115
polymer
www.elsevier.com/locate/polymer

Modeling of composite fiber production with silica nanoparticles dispersed in polyethyleneoxide

R. Furlan [a,*], E.W. Simões [b], M.L.P. da Silva [b,c], I. Ramos [a], E. Fachini [d]

[a] University of Puerto Rico at Humacao, Physics and Electronics Department, CUH Station, 100, 908 Road, Humacao, Puerto Rico 00791, USA
[b] Polytechnic School, University of São Paulo, Av. Luciano Gualberto 158, Trav.3, São Paulo, SP 05508900, Brazil
[c] Faculty of Technology of São Paulo, Pça Cel. Fernando Prestes, 30, São Paulo, SP 01124060, Brazil
[d] University of Puerto Rico at Río Piedras, Facundo Bueso Bldg., FB-B1, San Juan, Puerto Rico 00931, USA

Received 5 February 2007; received in revised form 15 June 2007; accepted 18 June 2007
Available online 23 June 2007

Abstract

In this work silica nanoparticles were incorporated in a polymeric matrix (fibers) aiming at the production of new composite materials that can be useful for the development of nanomaterials and/or microanalysis systems. Polyethyleneoxide and Ludox TM-50 were used as phases for electrospinning. Due to the high amount of effective charge present in the solutions, a new setup for electrospinning was devised by adding another electrode to a conventional deposition system. The presence of this electrode was investigated numerically using electrostatic application mode of the COMSOL Multiphysics 3.2b package. The simple model developed to explain the nanoparticle behavior for the used electrospinning setup showed good agreement with the experimental results and can be useful for simulations in the production of similar composites. Fibers with a high amount of particles were obtained using this third electrode biasing the flow in a preferred direction. Infrared spectra, EDX and SEM microscopy analysis show nanoparticle incorporation in the fibers.

Keywords: Composite; Nanoparticles; Fiber formation

1. Introduction

Invented in the 1930s, electrostatic deposition (or electrospinning) technique has recently gained significant interest because it can produce a variety of ultra fine polymer fibers in the micro or even nano-scale diameters at low cost [1–5]. Huang et al. [1] compared in detail this technique with others used to obtain polymeric fibers and, also, gave extensive information about the use of different types of polymers with electrospinning. Recent works have demonstrated the feasibility of obtaining alignment of fibers and structures (normally pads for electric contact) previously defined on the substrate [6,7].

A typical electrospinning process is depicted in Fig. 1 [1]. An electrostatic field is used to form and accelerate liquid jets from the tip of a capillary. The surface of a hemispherical liquid drop suspended in equilibrium at the end of the capillary will be distorted into a conical shape in the presence of the electric field. The balancing of the repulsive force, resulting from the induced charge distribution on the surface of the drop with the surface tension of the liquid, causes this distortion. Once a critical voltage is exceeded, a stable jet of liquid is ejected from the cone tip. For a sufficiently viscous liquid the jet travels to the grounded target and the solvent evaporates. Charged polymer fibers are formed and lay themselves randomly on the collecting metallic electrode.

It is well known that the morphology of the resulting fibers is determined by a synergetic effect of solution parameters and electrostatic forces [8–12]. These parameters include viscosity, surface tension, concentration and dielectric properties of the spinning solution and process parameters such as the feed rate of the solution to the tip and acceleration voltage. Controlling the process parameters, the fibers can be

* Corresponding author. Tel.: +1 787 8509381; fax: +1 787 8509308.
E-mail address: rfurlan@mate.uprh.edu (R. Furlan).

0032-3861/$ - see front matter © 2007 Elsevier Ltd. All rights reserved.
doi:10.1016/j.polymer.2007.06.041

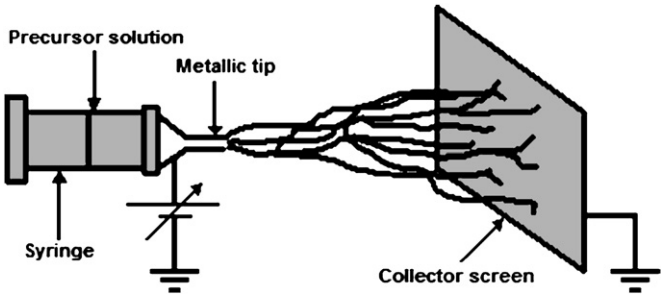

Fig. 1. Schematic diagram of an electrospinning process.

electrospun from different precursor solutions and their melts, like water-soluble polymers, biopolymers, suspensions containing particles, etc [1].

Silica nanoparticles present promising characteristics, such as good thermal and chemical resistance besides its relative biocompatibility, high surface area useful for catalytic purposes, and others [13–15]. All these properties strongly suggest the use of these particles in new materials development. However, up to now the use of silica nanoparticles for the development of microstructures for sample pretreatment in catalytic devices, has not being fully explored [16]. Moreover, although there are several methods to produce these microstructures, the use of electrospinning of an organic polymeric fiber to support these nanoparticles has not been attempted yet. Nonetheless, this possibility requires only two steps and consists of a simple method to distribute the particles saving their vast superficial area, which allows the better use of their catalytic properties [15].

Therefore, the aim of this work was to produce new composite materials, useful for the development of nanomaterials and/or microanalysis systems, using the electrospinning of dispersed organic and inorganic compounds in water, an environmentally mild solvent [17,18].

2. Experimental

2.1. Simulations

In order to understand the electrostatic interactions in the electrospinning setup, simulations were performed using COMSOL Multiphysics (FEMLAB) 3.2b [19] in a Pentium Dual Core platform (2.66 GHz, 4 GB of RAM). Fig. 2 shows the used design and mesh configuration (251,776 elements). The syringe is divided into two distinct parts: the metallic needle, which is considered inside the apparatus environment and may influence the electric field on the surroundings, and the body, which is not relevant to the electric field application. The surrounding environment is considered as a square area that contains the main parts of the setup. Table 1 describes the potentials applied and materials of the main parts of the experimental setup.

Electrospinning was usually processed using tens of kV of DC voltage applied to two electrodes (syringe needle and collector in Table 1) that are positioned tens of centimeters apart.

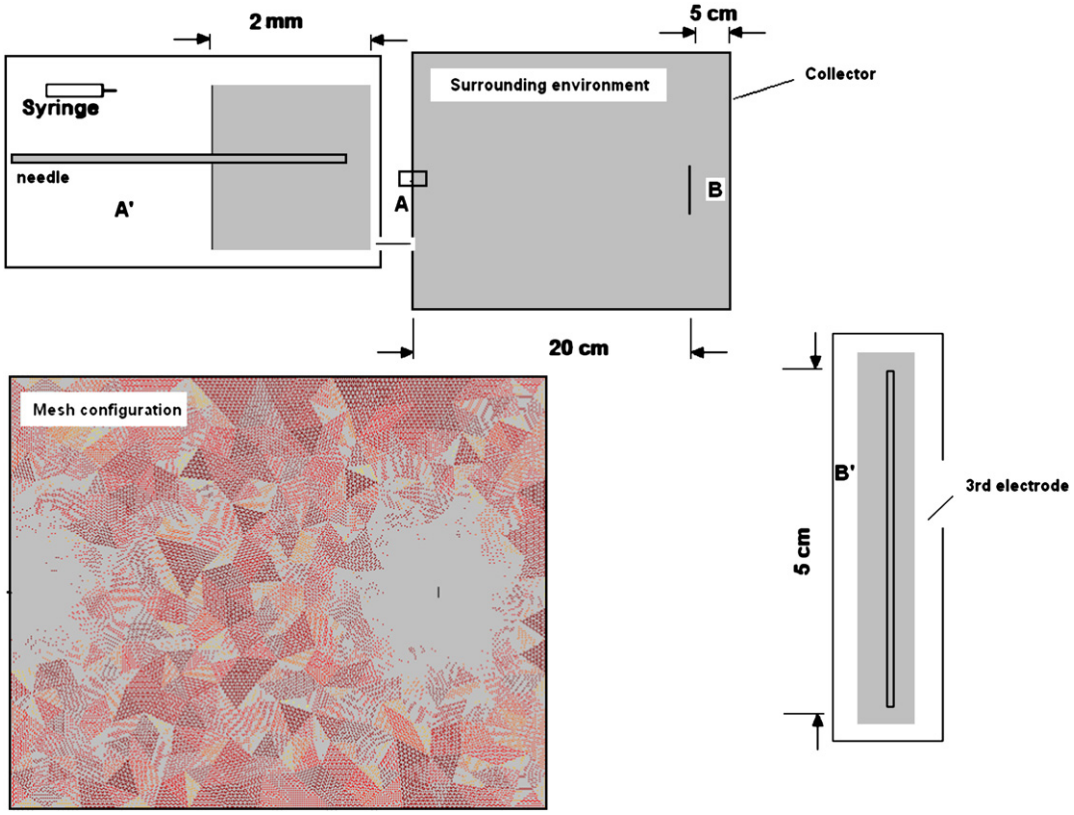

Fig. 2. Design and mesh configuration (251,776 elements) used in simulations with COMSOL Multiphysics.

Table 1
Potentials applied to the main parts of the experimental setup and materials

Setup parts	Material	Applied potential
Syringe needle	Stainless steel	±15 kV; ±35 kV
Collector	Stainless steel	0 V
Third electrode	Stainless steel	±500 V; ±250 V; 0 V, without electrode
Surrounding environment	Air	Floating or grounded

Since the nanoparticles require high amount of effective charges in order to be dispersed in water, the electrospinning might be hindered due to particle repulsion. Therefore, we propose the addition of a third DC voltage electrode to the setup in order to direct the nanoparticles, and, consequently, the obtained composite fibers. This is a small electrode positioned between the syringe and the collector screen.

The simulations were performed considering total number of charges 10^{12} or 10^{20} on the nanoparticles. The lower total charge corresponds to a very diluted solution containing silica nanoparticles and the higher total charge to a solution containing nearly 10% of silica nanoparticles dispersed in the solvent. Whereas the nanoparticles are negatively charged, because the surface corresponds to silicate ions, the solution itself is positively charged due to the presence of sodium ions as counter ions.

Finally, a homogeneous Neumann condition [20,21] was assumed for all simulations, unless another condition was specified.

2.2. Materials and methods

The reactants are (a) polyethyleneoxide (PEO) (molecular weight: 2,000,000), (b) Ludox TM-50 (a commercial suspension of silica nanoparticles) from Aldrich Co., (c) a buffer solution (pH 10.00; color-coded blue − potassium carbonate/potassium tetraborate/potassium hydroxide/disodium EDTA dihydrate), (d) ethanol, and (e) isopropanol, all from Fisher Sci. All solutions used deionized water. Silicon wafers were used as substrates for fiber deposition.

The solutions were analyzed by infrared spectroscopy on the transmission mode while the thin films on silicon wafers, obtained by spinning (1000 rpm, 45 s), were analyzed by the attenuated total reflectance (ATR) mode. Fibers' dimensions and morphology were determined by optical and scanning electron microscopy (SEM). The chemical composition of these fibers deposited on silicon was obtained using the SEM EDX module or infrared using the ATR mode.

3. Results and discussion

3.1. Simulations

The electrospinning process requires the formation of Taylor's cone [22]. This effect depends on several parameters, one of the particular relevance being the electric potential applied to the syringe needle. The influence of the electric field is even more significant if charged particles and polar solvents or polymers are used, due to their electric repulsion.

Considering the conditions presented in Table 1, typical simulation results (presented in Fig. 3) reveal that the elliptical shape of the equipotential lines, which favors the formation of Taylor's cone, can be observed only if the equipotential lines in the surrounding environment end at the base of the syringe needle, Fig. 3a and a′ (detail). Equipotentials ending at the needle outlet, Fig. 3c and c′, corresponds to a condition where a strong perturbation, such as a different material, electrically grounded, is placed at the surrounding surface, which may distort the shape of the Taylor's cone and the drop that forms the fiber. An intermediate state is found in Fig. 3b or b′ and corresponds to a perturbing object placed in the middle of the needle.

A perturbing electric field in front of and near the outlet of the syringe needle was added to the simulation, by the addition of an array of negatively charged particles (100 elements, elliptical shape, maximum size of 20 μm, distance from the needle outlet = 150 μm, 10^3 total number of charge/each element). This condition corresponds approximately to a cloud of nanoparticles frozen immediately after the ejection from the needle. Typical results are presented in Figs. 4 and 5. As can be seen in Fig. 4, the maximum disturbance of the electrical field is found for surroundings with floating potential, since the nanoparticles array does not allow the electric field to penetrate the base in the direction of the grounded electrode. However, this shielding effect is reduced for grounded surroundings, as presented in Fig. 5.

Note how this simple and qualitative model allows for a better understanding of the influence of charged particles in the fibers' formation process.

In order to compensate for the disturbance caused by the highly charged particles in the simulations, a third (small) electrode was added to the system, as described earlier. For all conditions it was assumed that the equipotentials through the environment ends at the base of the needle, as shown in Figs. 3a and 4a, which represent less disturbed conditions. Figs. 6–9 show the electric field streamlines (perpendicular to the equipotentials) with or without the additional electrode, as a function of the potential in the surrounding environment. As can be seen in Fig. 6, there is no meaningful difference between floating and grounded environment if the third electrode is not used. Similar results can be obtained using negative potentials or higher values such as +35 kV.

With the addition of the third electrode, which corresponds to an electrostatic lens and a disturbance to the grounded condition, the electric field is highly dependent on the surrounding conditions. For grounded surrounding conditions, as shown in Figs. 7 and 8, the addition of the third electrode plays an important role even at 0 V but does not show any dependence on needle potential. Applying a potential of 0 V at the third electrode it acts as a convergent lens, that orients and/or confines (focus) the electric field (Figs. 7b and 8b). If the electrode potential is opposite to that of the needle (Figs. 7c and 8a), the electrode acts as a more potent lens, which allows for divergence. Finally, with an equivalent charge accumulation

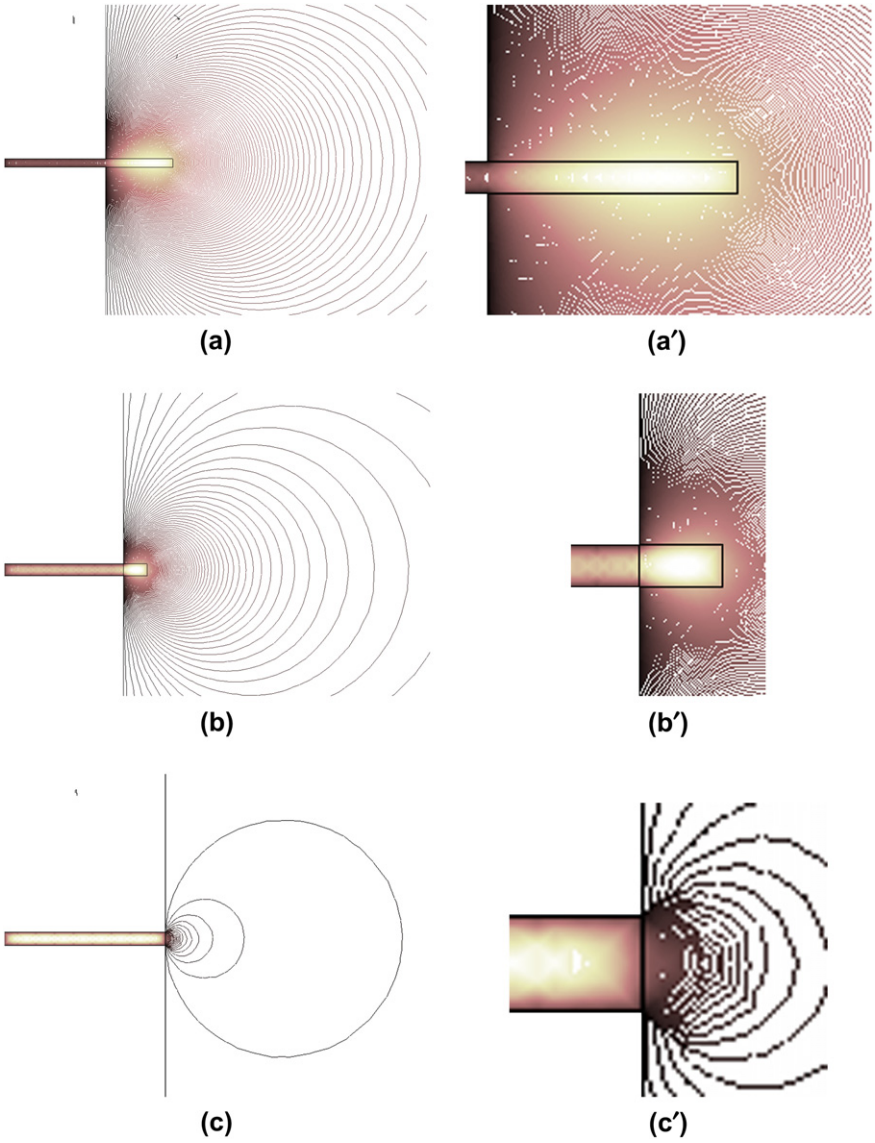

Fig. 3. Equipotential lines for a not grounded surrounding environment (floating potential) ending at (a, a′) the base, (b, b′) the middle and (c, c′) the outlet of the syringe needle. Potential applied to the syringe was +15 kV and surroundings with floating potential.

(potential) (Figs. 7a and 8c) repulsion occurs and a high divergent lens is obtained between the needle and the third electrode.

For floating surrounding environment, or even with a grounded electrode much bigger than the third electrode as presented in Fig. 9, any set of parameters displays a similar result and the typical solution is shown in Fig. 9a. Therefore, the third electrode always allows for directing the electric field.

However, if a severe perturbation in the needle outlet occurs, e.g. a non-homogeneous Neumann condition, the third electrode no longer acts as a convergent electrostatic lens (Fig. 9b). On these conditions a Taylor's cone probably will not be formed.

The numerical simulations point out the use of a third electrode in order to orient the electric field, which creates preferential paths for the charged nanoparticles slurry throughout the chaotic process of electrospinning. Thus, an array of nanoparticles, similar to the one used previously, was simulated using the conditions in Fig. 9. The obtained results are the same for both surrounding environment conditions and the typical equipotential lines are shown in Fig. 10.

This last result is quite similar to the one obtained in Fig. 4 and shows that the third electrode plays an important role once the field is oriented so it passes through it on both conditions. Considering the results obtained, a setup including the third electrode was built and fibers were deposited using silica nanoparticles dispersed on PEO.

3.2. Fiber formation

There are some constraints to the complete mixture of the reactants and consequently to obtain one stable slurry of PEO with dispersed silica nanoparticles (Ludox), such as (a) the stability of Ludox dispersion is quite dependent on pH

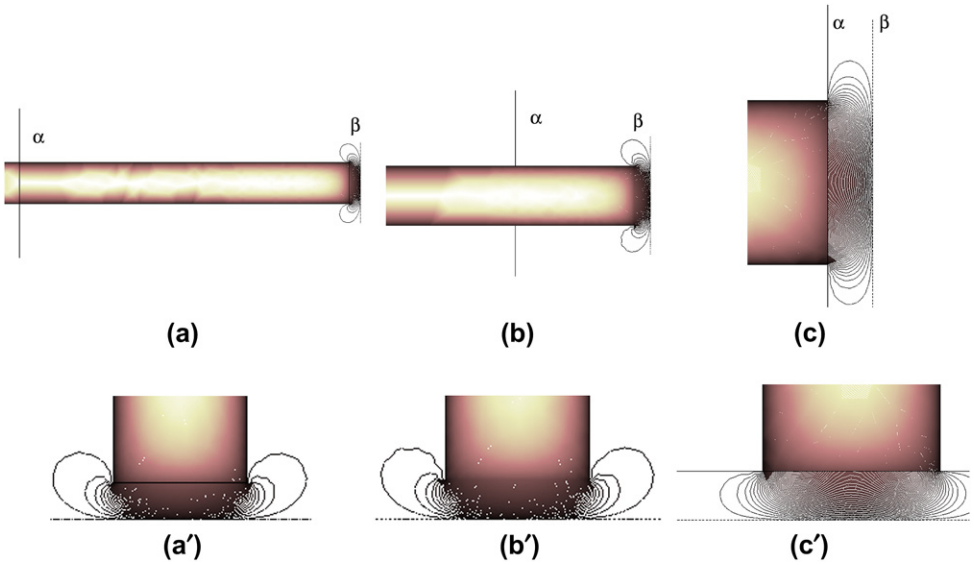

Fig. 4. Equipotential lines for a floating potential ending at (a, a′) the base, (b, b′) the middle and (c, c′) the outlet of the syringe needle, with charged particles disturbing the outlet of the needle surroundings. Potential applied to the syringe was +15 kV and surroundings with floating potential. α is the surrounding environment; β is the array of charged particles.

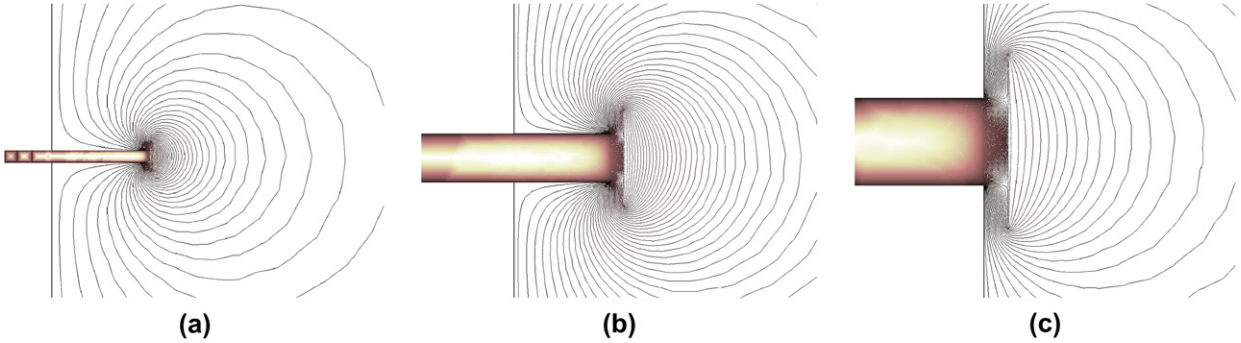

Fig. 5. Equipotential lines for a floating potential ending at (a) the base, (b) the middle and (c) the outlet of the syringe needle, with charged particles disturbing the outlet of the needle surroundings. Potential applied to the syringe was +15 kV and grounded surroundings.

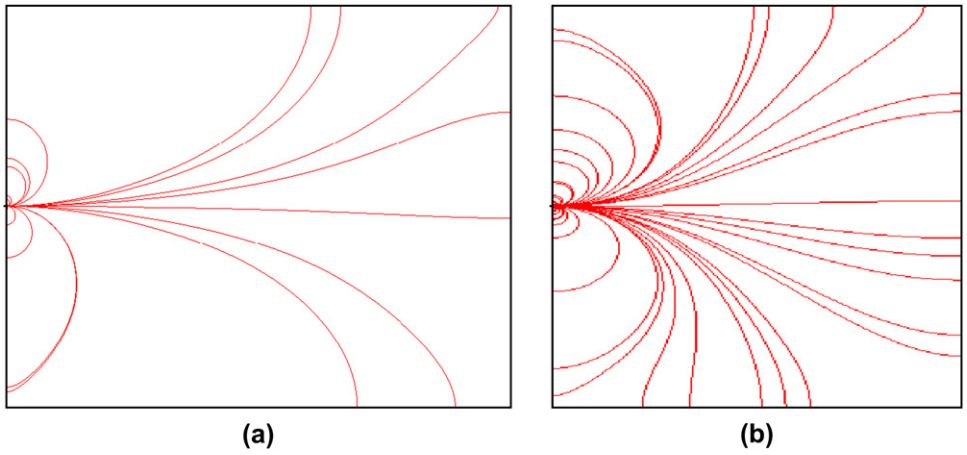

Fig. 6. Electric field streamlines for a setup without the third electrode, as a function of the surrounding environment potential. Syringe needle potential was +15 kV and total space charge of 10^{20}. (a) Grounded; (b) floating.

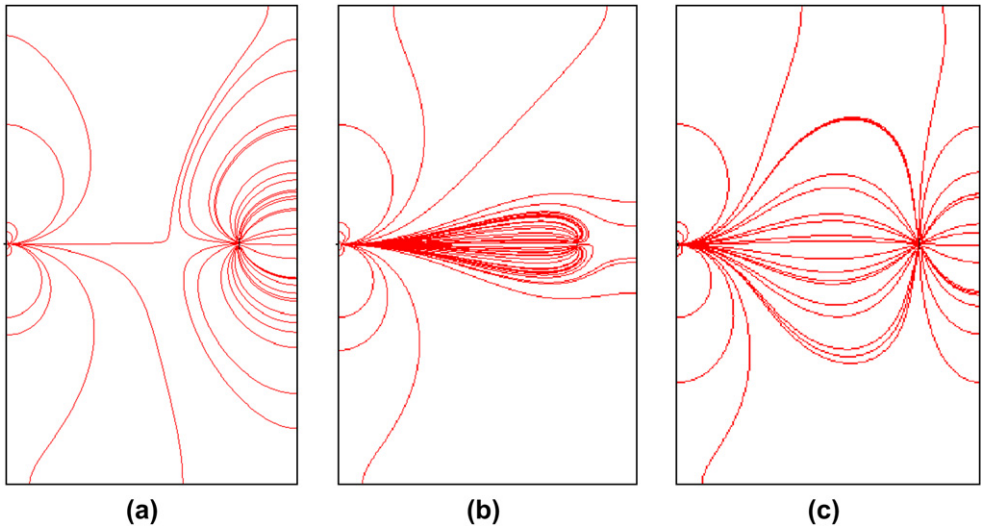

Fig. 7. Electric field streamlines for a setup including the third electrode. Syringe needle potential of −35 kV, surrounding environment grounded, and total space charge of 10^{20}. Additional electrode at (a) −500 V; (b) 0 V; (c) +500 V.

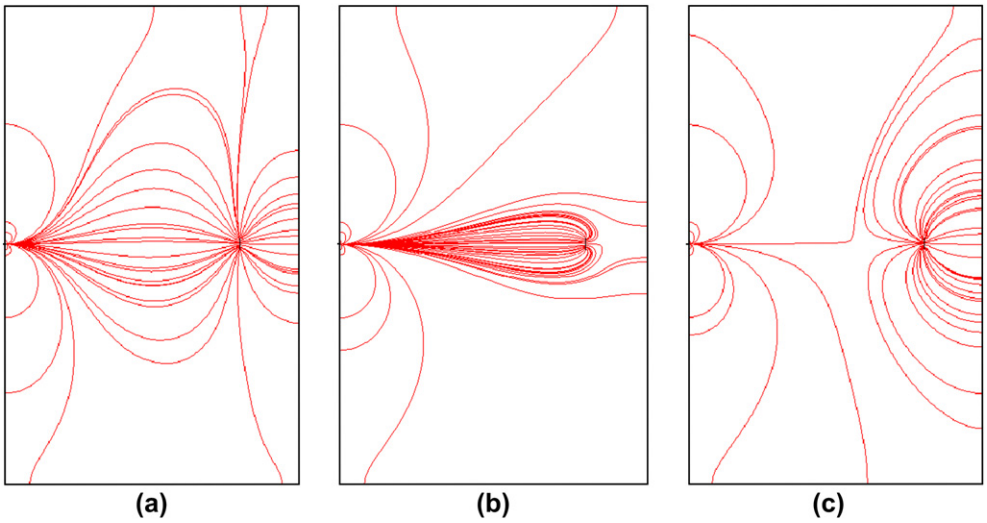

Fig. 8. Electric field streamlines for a setup including the third electrode. Syringe needle potential of +35 kV, surrounding environment grounded, and total space charge of 10^{20}. Additional electrode at (a) −500 V; (b) 0 V; (c) +500 V.

and ionic activity; (b) homogeneity of the PEO emulsion depends on the experimental manufacturing procedures, e.g. heating. In order to obtain stable dispersions, the following parameters were evaluated: (a) PEO and/or Ludox concentration; (b) solvent polarity, using water, ethanol and isopropanol; (c) ionic activity using pH 10.00 buffer solution and (d) heating.

Table 2 summarizes data obtained by infrared analysis of slurries and/or dispersions using different solvent polarity, polymer and particle concentration. Bands were measured mainly at a wavenumber of 2880 cm^{-1} (CH_n), 1150 cm^{-1} and 1050 cm^{-1}. The intensity at 1050 cm^{-1}, corresponding to Si−O−Si groups from silica, was used as a nanoparticles' concentration index in the composite film. On the other hand, the amount of polymer was evaluated by the integrated intensity of the band at 1150 cm^{-1}. Despite proximity in the spectra, Fig. 13 shows that the interference of one band over the other, in the fiber samples, is not qualitatively significant and does not demand correction. Under those circumstances, the ratio Si−O−Si/C−O was used as a parameter to evaluate the composition of the final samples. For ethanol, the position of the CO band has to be considered due to the organic solvent contribution.

As can be see in Table 2, due to its characteristics, ethanol samples do not favor particle dispersion. For a similar PEO concentration, the increase in the relative intensity due to the buffer solution, most likely is due to the increase in ionic activity.

In general, in a much-diluted concentration (<10 wt%) the nanoparticles can be stable in water, and mixtures of water and alcohol even in concentrated PEO slurries (10 wt%). The use of buffer solutions favors dispersion, but diminishes the amount of nanoparticles that can be introduced in the slurry.

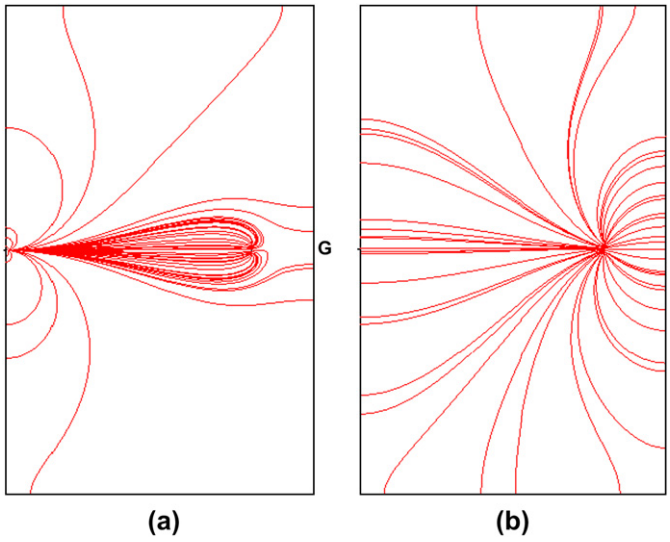

Fig. 9. Electric field streamlines as a function of surrounding environment. Syringe needle potential of ±15 kV or ±35 kV. (a) Floating surrounding environment or grounded frontal wall (G); positioned as in Fig. 4a and additional electrode at 0 V or ±500 V; (b) floating surrounding environment positioned as in Fig. 4a and additional electrode at 0 V, or ±500 V in a non-homogeneous Neumann condition.

The use of organic solvents shows similar behavior. Moreover, buffer solutions may lead to nanoparticles' precipitation after 24 h resting. Heat favors the formation of PEO slurries but does not preserve the nanoparticles suspended in that slurry. Therefore, the PEO solutions were prepared and the nanoparticles were added immediately before use. The most stable dispersions are 1 wt% PEO, 1 wt% silica nanoparticles in water or in buffer solution. XRD analysis of PEO solutions, with or without nanoparticles, did not show any difference, indicating a low probability of nanoparticles' aggregation. Fig. 11 shows a typical analysis of these dispersions and also of Ludox TM-50, for comparison.

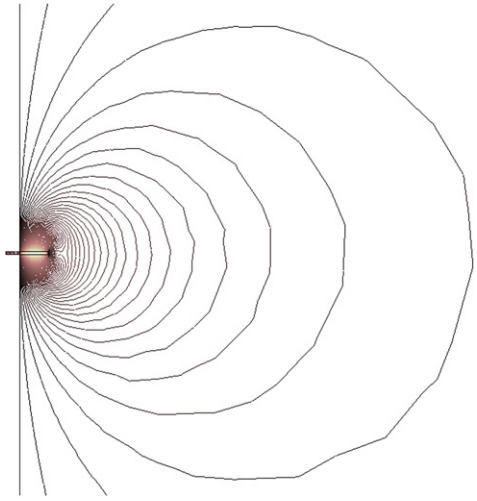

Fig. 10. Equipotential lines near the needle considering the disturbance caused by the presence of charged particles. Potential applied to the syringe was +15 kV.

Table 2
Relative intensity for Si–O–Si/C–O bands obtained by infrared analysis of emulsions and/or dispersions using different solvent polarity, polymer and particle concentration

Sample conditions			Si–O–Si/C–O relative intensity
Concentration (g PEO/g solvent)	Solvent	Nanoparticles/PEO weight proportion	
0.0056	Ethanol	1:1	0.08
N.A.	Water	1:0	0.05
0.080	Water	1:1	0.31
0.012	Water	1:1	0.35
0.012	Water	1:2	0.39
0.017	Water	1:1	0.19
0.015	Buffer solution	1:1.3	0.23

N.A.: not applicable.

Emulsions or dispersions with water or buffer solution as solvents were used to make fibers in the setup previously described and simulated. The voltages used were 0 V, ±100 V and ±250 V (from the third electrode to the ground). The use of a third electrode and positive or negative voltage drives

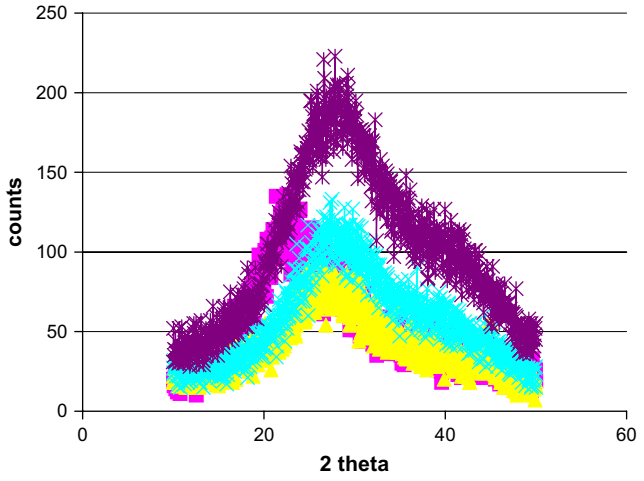

Fig. 11. XRD analysis: ■ – Ludox TM-50 only; X – PEO emulsion only; ★ – Ludox (1 wt%) + PEO (1 wt%) using buffer solution as the solvent; ▲ – Ludox (1 wt%) + PEO (1 wt%) using water as the solvent.

Table 3
Fiber morphology determined by optical microscopy

Dispersion	Applied voltage on third electrode (V)		
	−250	0	+250
PEO (0.01 wt%) + Ludox (0.01 wt%) in water	Thin fibers, smooth surface	Mainly drops	Thick fibers, smooth surface
PEO (0.01 wt%) + Ludox (0.01 wt%) in buffer solution	Thin fibers, rough surface	Fibers and drops, rough surface	Thin fibers, rough surface
Pure PEO (0.01 wt%) emulsion in water	Thin fibers, smooth surface	Mainly drops, smooth surface	Drops, smooth surface
Pure Ludox TM-50 dispersion + PEO (0.01 wt%)	Drops	Drops	Drops

the flow straight, whereas voltage zero allows for some flow divergence. However, the removal of the third electrode produces a condition where the flow can spread completely around the environment but is preferentially driven to the nearest grounded surface. No meaningful difference between ±100 V and ±250 V was observed. These results are in good agreement with simulations for a condition with floating surroundings (Fig. 9a) that better corresponds to our experimental conditions, although the proximity of grounded parts cannot be ignored as they may explain the occurrence of some fiber flow divergence for 0 V applied to the third electrode.

Table 3 summarizes the morphology differences found on deposited fibers using optical analysis if a PEO (0.01 wt%) + Ludox (0.01 wt%) dispersion is electrospinned. The case of 0 V did not seem adequate to drive the nanoparticles in the direction of the third electrode, as only drops can be collected on the surface of this electrode. High levels of charges hinder the fiber formation and the Ludox dispersion only shows the formation of drops, not fibers, on the third electrode. The buffer likely allows for a better distribution of the nanoparticles inside the fibers and therefore, a rough surface is obtained.

SEM analysis showed differences on the fiber surfaces accordingly if the solution or dispersion was used. Fig. 12 shows typical results with the third electrode at −250 V. For the PEO water emulsion (Fig. 12a), it is possible to observe a smooth surface even near a bead and the same is noticed for PEO buffer emulsion (Fig. 12b), although this emulsion leads to much bigger beads. PEO + nanoparticles dispersed on buffer (Fig. 12c) shows a rough surface, most likely due to the presence of nanoparticles. Also, infrared analysis shows silica particles inside the fibers as can be seen in Fig. 13. In this figure, the infrared

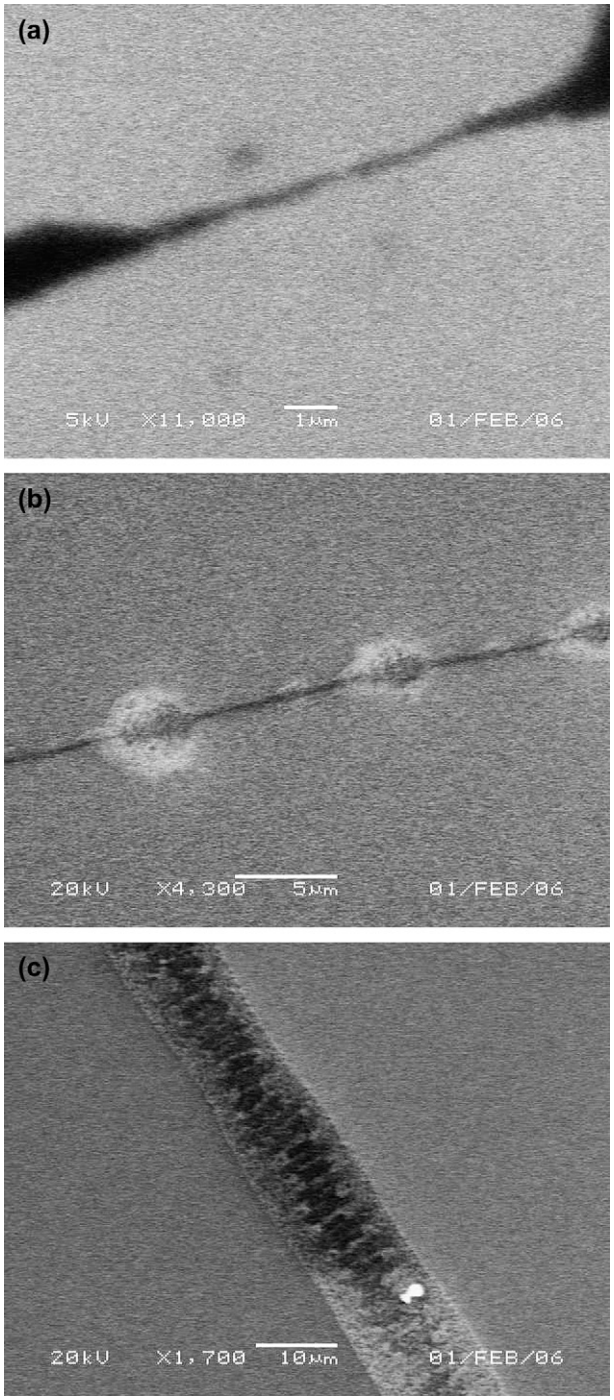

Fig. 12. SEM analysis: (a) PEO water emulsion; (b) PEO buffer emulsion and (c) PEO + nanoparticles dispersion. All conditions with the third electrode at −250 V.

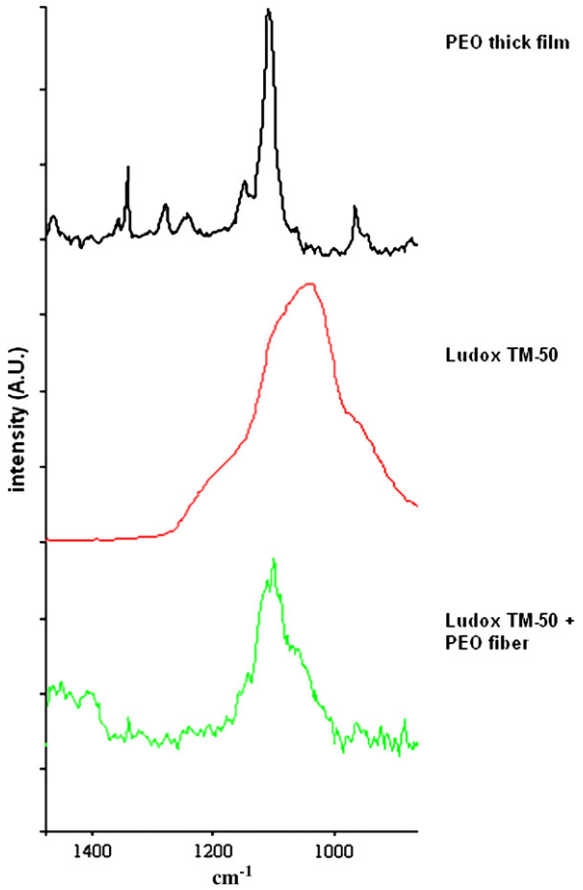

Fig. 13. Infrared spectra of PEO thick films, Ludox dispersion and fibers produced with PEO (0.01 wt%) + Ludox (0.01 wt%) and buffer solution as solvent.

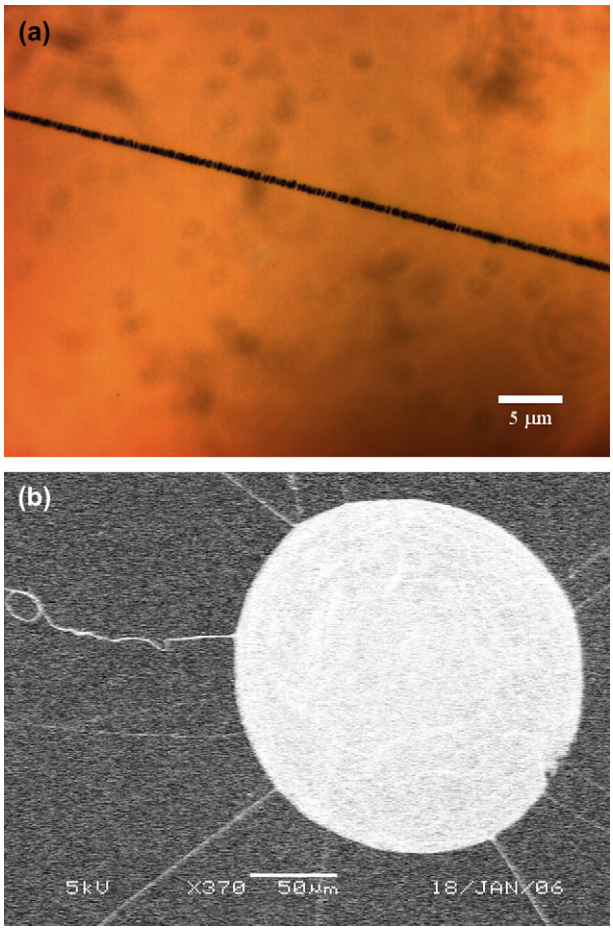

Fig. 14. Particles formed with electrospinning process in a (a) dispersion of nanoparticles in PEO water emulsion (optical microscopy) and in a (b) viscous emulsion (SEM analysis).

spectrum of the fibers shows bands that can be assigned to Ludox and PEO.

Highly viscous dispersions (10 wt% PEO, 3 wt% silica nanoparticles in water) also lead to fiber formation. Some of these fibers may present particles inside, as can be seen in Fig. 14a. It is possible to observe in Fig. 14a that several particles aligned inside a fiber. Nonetheless, nanoparticles easily aggregate and produce clusters as big as 200 μm, as can be seen in Fig. 14b. EDX analysis of the large clusters presented in Fig. 14b shows atomic ratio of 1:1 to Si:O whereas the silicon substrate presents 1:0.1. This fact indicates that the large cluster is formed by coalescence of silica particles. The spherical format and big size suggest that the clusters are formed during electrospinning process.

4. Conclusion

The simple and qualitative model used to simulate the use of a third electrode shows a good agreement with the experimental results and can be used to guide other composite production.

We demonstrated, experimentally and by simulation, the advantages of using electrospinning, a simple procedure, to obtain nanoparticles dispersed on polymeric fibers. Due to the high amount of effective charges on the dispersion used, an adaptation of the electrospinning setup was needed, and the new composite formed can be useful for several applications, such as sample pretreatment for chemical analysis.

Acknowledgment

We acknowledge the financial support of CNPq and FAPESP, in Brazil, and also NSF-DMR-0353730 and NSF-SBE-0123654.

References

[1] Huang ZM, Zhang YZ, Kotaki M, Ramakrishna S. Composite Science and Technology 2003;2223–53.
[2] da Silva ANR, Furlan R, Ramos I, da Silva MLP, Fachini E, Santiago-Aviles JJ. Electrochemical Society Proceedings 2003;2003–2009: 284–91.
[3] Doshi J, Reneker DH. Journal of Electrostatics 1995;35:151–9.
[4] Formhals A. U.S. Patent 1,975,504; 1934.
[5] Larrondo L, Manley RS. Journal of Polymer Science. Part B: Polymer Physics 1981;19:933.
[6] Kameoka J, Craighead HG. Applied Physics Letters 2003;83(2):371–3.
[7] Li D, Wang Y, Xia Y. Nano Letters 2003;3(8):1167–71.
[8] Reneker DH, Yarin AL, Fong H, Koombhongse S. Journal of Applied Physics 2000;87(9):4531–47.
[9] Hendricks CD, Schneider JM. American Journal of Physics 1963;31:450–3.
[10] Taylor GI. Proceedings of the Royal Society London Series A 1969; 313:453–75.
[11] Inculet II, Fischer JK. IEEE Transaction on Industry Applications 1989;25(3):558–62.
[12] Baumgarten PK. Journal of Colloid and Interface Science 1971; 36(1):71–9.
[13] Choi SS, Lee SG, Im SS, Kim SH, Joo YL. Journal of Materials Science Letters 2003;22:891–3.
[14] Wang ZL, Gao RP, Gole JL, Stout JD. Advanced Materials 2000; 12(24):1938–40.
[15] Gole JL, Stout JD, Rauch WL, Wang ZL. Applied Physics Letters 2003;76(17):2346–8.
[16] Carvalho RAM, Lima RR, Filho APN, da Silva MLP, Demarquette NR. Sensors and Actuators B 2005;108:955–63.
[17] Murphy PE, Kangun N, Locander WB. Journal of Marketing 1978;42(4):61–6.
[18] Madu CN. Managing green technologies for global competitiveness hardback: Quorum Books; 1996. 280 pp. ISBN: 0-899-30827-9.
[19] COMSOL Multiphysics 3.2b © 1997–2006, COMSOL, Inc. http://www.comsol.com.
[20] Poppner M, Sonnenschein R, Meyer J. 10th International Conference on Electrostatics. Journal of Electrostatics 2005;63(6–10):781–7.
[21] Meyer J, Marquard A, Poppner M, Sonnenschein R. Electric fields coupled with ion space charge. Part 1: measurements. Journal of Electrostatics 2005;63:775–80.
[22] Taylor G. Proceedings of the Royal Society London Series A 1964;280:383.